

1 **Comparative Study of Deep Generative Models on** 2 **Chemical Space Coverage**

3 *Jie Zhang*^{&,§,||}, *Rocío Mercado*^ε, *Ola Engkvist*^ε, *Hongming Chen*^{&,||,*}

4 [&]Guangdong Provincial Key Laboratory of Laboratory Animals, Guangdong Laboratory
5 Animals Monitoring Institute, Guangzhou, 510663, P. R. China

6 [§]State Key Laboratory of Respiratory Disease, Guangzhou Institutes of Biomedicine and Health,
7 Chinese Academy of Sciences, Guangzhou 510530, P. R. China

8 ^{||}Bioland Laboratory (Guangzhou Regenerative Medicine and Health - Guangdong
9 Laboratory), Guangzhou 510530, P. R. China

10 ^εHit Discovery, Discovery Sciences, R&D, AstraZeneca, Gothenburg 43183, Sweden

11 *Correspondence e-mail: chen_hongming@grmh-gdl.cn

12 **Abstract**

13 In recent years, deep molecular generative models have emerged as novel methods for *de novo*
14 molecular design. Thanks to the rapid advance of deep learning techniques, deep learning
15 architectures such as recurrent neural networks, variational autoencoders, and adversarial networks,
16 have been employed for constructing generative models. However, so far the metrics used to
17 evaluate these deep generative models are not discriminative enough to separate the performance
18 of various state-of-the-art generative models. This work presents a novel metric for evaluating
19 deep molecular generative models; this new metric is based on the chemical space coverage of a

20 reference database, and compares not only the molecular structures, but also the ring systems and
21 functional groups, reproduced from a reference dataset of a 1M subset of GDB-13. The
22 performance of 7 different molecular generative models was compared by calculating their
23 structure and substructure coverage of the GDB-13 database while using the 1M subset for training.
24 The result shows that the performance of various generative models varies significantly using the
25 benchmarking metrics introduced herein, such that generalization capability of the generative
26 model can be clearly differentiated. Additionally, the coverage of ring systems and functional
27 groups existing in GDB-13 was also compared between the models. Our study provides a useful
28 new metric that can be used for evaluating and comparing generative models.

29 **Introduction**

30 Deep learning has been successfully used in many fields to learn relationships that are too complex
31 to learn using traditional computer algorithms, including early image classification,^{1,2} facial
32 recognition, and music recognition.³ Deep learning even surpasses the performance of human
33 experts in some challenging tasks, such as playing GO.⁴ Moreover, deep generative models play
34 important roles in tasks like music composition,⁵ image generation,⁶ and language translation.⁷ In
35 the last five years, deep generative modeling has also been applied in the fields of cheminformatics
36 and molecular design. One interesting example is using deep neural networks for compound
37 structure generation.⁸⁻¹¹

38 The number of chemically feasible, drug-like molecules has been estimated to be on the order of
39 $10^{60} - 10^{100}$ compounds.¹² For such a large chemical space, it is clearly impossible to synthesize and
40 test every compound for pharmaceutical applications. To efficiently explore the space, molecular

41 generative models have emerged in recent years with the aim of better navigating through this
42 huge chemical space for *de novo* molecule design.

43 *De novo* molecular design has long been put forward as a way to accelerate the drug discovery
44 process as it is expected to save time and resources in drug discovery, where it can take over a
45 decade and billions of dollars in investment to bring a single drug to market.¹³ Historically, *de novo*
46 design methods have been mainly rule-driven and used brute force algorithms to achieve their
47 goal.¹⁴ For example, creating a virtual library using fixed rules and building blocks, then scoring
48 each compound in the virtual library to find the best compound. Genetic algorithm based
49 algorithms were also proposed to tackle the *de novo* design issue.^{15,16} In contrast, deep generative
50 molecular design is the concept of generating molecules using deep neural networks. Deep
51 generative models are data-driven methods which generate compound structures by learning the
52 underlying probability distributions in a compound dataset instead of screening existing databases
53 for molecules that fit the desired profile. Deep generative models are powerful as they allow
54 chemists to bypass models using hard-coded chemical rules which do not scale to larger datasets.
55 Furthermore, not all chemical rules are easy to define. Using deep generative models, one can
56 avoid enumerating all possible structures for a given application and then screening them (a
57 daunting task). Instead, one can simply train a model using known compounds, and sample the
58 model for the desired set of properties (e.g. ADMET profile) to get out promising structures. *De*
59 *novo* generative models can generate structures that are in significantly narrower, but more
60 promising, regions of chemical space. Moreover, deep learning methods can take advantage of all
61 the information available in ever-increasing large public datasets, thanks to automation
62 technologies used in high-throughput screening and parallel synthesis.¹⁷

63 In recent years, many molecular generative models have been published, such as CharRNN, VAE,
64 and REINVENT, which are remarkable at sampling molecules both in- and outside the training set
65 used to learn chemistry rules.^{11,18-21} It is worth noting that CharRNN was introduced as a general
66 language model at the first place. However, similar architectures are also successfully applied in
67 molecular generative models, e.g. REINVENT adopted a similar architecture with reinforcement
68 learning.²²⁻²⁶ VAE is a general architecture that has a wide range of applications in many generative
69 models and tasks.²⁷⁻²⁹ In current study, we adopts the implementation of CharRNN and VAE
70 provided by the MOSES.¹⁰ Notably, many of these generative models have been benchmarked
71 using existing “distribution-based” metrics implemented in open-source programs such as
72 MOSES¹⁰ or GuacaMol.³⁰ However, these metrics are in general non-discriminative as many of
73 these state-of-the-art (SOTA) models perform quite well across all the included metrics, such that
74 it is difficult to compare them and gain a deep understanding of each model’s strengths and
75 weaknesses. We previously proposed a new metric: the percent coverage of functional groups
76 present in GDB-13.³¹ As an extension of our previous work,³² we apply the idea as a way for
77 benchmarking the performance of multiple generative models. GDB-13 contains in total
78 975,820,210 structures, which enumerate small organic molecules containing up to 13 atoms of C,
79 N, O, S, and Cl by following simple chemical stability and synthetic feasibility rules.³² The
80 generalization capability of deep generative models is assessed by computing how much of the
81 whole GDB-13 can be recovered by a model trained from a small GDB-13 subset.

82 Substructure has long been used to characterize the composition of compounds. One concept is
83 the so-called *functional group*, frequently used in many fields in chemistry, including medicinal
84 chemistry. A functional group is defined as a subset of connected atoms in a molecule that in some
85 way endows specific intrinsic properties (or *functions*) to a molecule. Furthermore, the presence

86 or absence of a functional group in a molecule could determine whether a molecule will react in a
87 given reaction. Some of the most common groups in medicinal chemistry include amides
88 ($\text{RC}(=\text{O})\text{NR}'\text{R}''$), ethers ($\text{R}-\text{O}-\text{R}'$), and amines ($\text{RR}'\text{NR}''$), where R, R', and R'' represent organic
89 groups or hydrogen atoms.³³ Another substructure-based concept is the *ring system*; ring systems
90 are the key components of molecular scaffolds. They play an important role in a molecule's
91 observed properties, such as the electronics, scaffold rigidity, molecular reactivity, and toxicity.
92 On average six new ring systems enter the drug space each year and approximately 28% of new
93 drugs contain a new ring system.³⁴ We investigated the percentage of chemical space covered in
94 terms of full structures, functional groups, and ring systems by published SOTA generative models.
95 The size of GDB-13 was hypothesized to be large enough to highlight differences between the
96 various models.

97 Four major classes of deep generative models are benchmarked and studied in this work, including
98 those based on recurrent neural networks (RNNs), autoencoder (AE) based networks, generative
99 adversarial networks (GANs), and graph neural networks (GNNs). The deep generative models
100 based on RNNs include REINVENT^{18, 32, 35} and CharRNN,²⁵ which use SMILES as the input and
101 output strings. VAE,³⁶ AAE,^{21, 37} ORGAN,²⁰ and LatentGAN¹¹ adopt either an AE or GAN for structure
102 generation using SMILES. Besides the SMILES-based generative models, one graph-based
103 generative model, GraphINVENT,³⁸ which uses GNNs in its core architecture, is also included in
104 the benchmark study. An effort was made to cover most of the major types of generative model
105 architectures in this study, in the hope that this would provide a comprehensive comparison for
106 existing generative models.

107 **Methods**

108 **Extraction of functional groups and ring systems.** To identify functional groups (FG) in the
109 various sets of molecules in this work (generated molecule sets, and GDB-13), the RDKit
110 functional group identification package,³⁹ which is based on an algorithm introduced by Peter Ertl
111 for automatically identifying functional groups, was used.⁴⁰ The advantage of the method is that it
112 is not based on manually curated lists of functional groups, and thus can be applied to any chemical
113 series. It is important to note that different chemists have slightly different definitions of what is a
114 functional group; however, as the benchmark introduced here calculated ratios of functional groups
115 in the generated and reference sets, a difference in opinions between chemists shouldn't be relevant.
116 The extraction of compound ring system (RS) was done using RDKit. First, all monocyclic rings
117 were retrieved; monocyclic rings were then fused depending on if individual ring systems shared
118 atoms or not.

119 **Generative models.** The models studied in this study include CharRNN, REINVENT, AAE, VAE,
120 ORGAN, LatentGAN, and GraphINVENT. The REINVENT code available at the
121 github.com/undeadpixel/reinvent-randomized repo^{35,41} was used; the CharRNN, AAE, VAE, and
122 ORGAN codes available at the MOSES GitHub repository^{10,42} were used; the LatentGAN code
123 available at the github.com/Dierme/latent-gan repository^{11,43} was used. Unlike original implement
124 of LatentGAN, we retrained the embedded Deep Drug Coder (DDC) model with randomly
125 selected 3M molecules from GDB-13 as the encoder and decoder component of LatentGAN. The
126 DDC code available at the github.com/pcko1/Deep-Drug-Coder repository⁴⁴ was used; finally, the
127 GraphINVENT code available at the github.com/MolecularAI/GraphINVENT repository^{38,45,46} was
128 used. All methods except for GraphINVENT are string-based generative models, whereas
129 GraphINVENT is a graph-based generative model.

130 **Training.** The GDB-13 database is used as the reference chemical space for this study.³¹ A one
131 million (1M) molecule subset of GDB-13 was randomly selected and used as the training set for
132 all the generative models. Another 200K molecules of GDB-13 were selected as the validation set
133 for calculating the validation loss. During training, a check point model was saved at every epoch.
134 The check point model with the lowest validation loss was chosen as the final model for sampling
135 1 billion (1B) SMILES.

136 **Hyperparameters.** For REINVENT, hyperparameters were taken from the GitHub repo.⁴¹ For
137 CharRNN, AAE, VAE, and ORGAN, the parameters were taken from the models' config file in
138 MOSES GitHub repo without further optimization. For LatentGAN, , the default values of
139 parameters in the GitHub repo were adopted.^{11, 43} For GraphINVENT, parameters and
140 hyperparameters for the best performing model (cGGNN) in the original publication were used
141 and not further optimized.⁴⁶ Detailed hyperparameters for each model can be found in SI Table S2.

142 **Sampling.** Once each model was trained, 1B compounds were sampled from each trained model.
143 The functional groups and ring systems were then identified for all sample sets as well as the full
144 GDB-13 set. All compounds in the analysis were standardized by converting to RDKit canonical
145 SMILES. Molecular graphs generated using GraphINVENT were further sanitized via
146 canonicalizing and aromatizing during the conversion to canonical RDKit SMILES for a more
147 fair comparison to the other models.

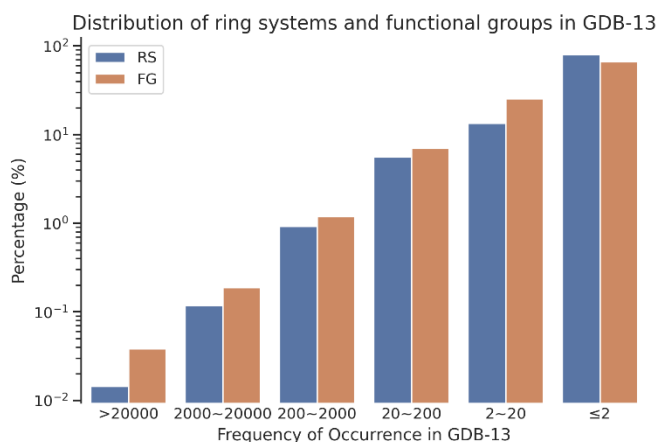
148 **Technical details.** For models in the MOSES repository and REINVENT, the training was done
149 using Python 3.6⁴⁷ and PyTorch 1.4⁴⁸. To accelerate sampling for 1B SMILES, the largest batch size
150 allowed by the GPU memory was adopted; for example, ORGAN, AAE, and VAE adopted a
151 sampling batch size of 25, 000, and CharRNN adopted a sampling batch size of 20,000. Also,
152 LatentGAN was trained using tensorflow-gpu 2.2, which adopted a sampling batch size of 50,000.

153 All the computations were performed on Linux workstations with GeForce RTX 2080Ti graphic
154 cards using CUDA 10.1. Canonical SMILES and dataset analysis were carried out using RDKit.³⁹
155 The Wasserstein distances⁴⁹ between distributions in Figure 2 were calculated with an in-house
156 script using SciPy.⁵⁰ Finally, GraphINVENT runs using Python 3.6 and PyTorch 1.2.

157 Results and Discussions

158 Analysis of the GDB-13 database

159 GDB-13 contains theoretically drug-like compounds whose heavy atom count is less than or equal
160 to 13 and, in total, comprises of 975,820,210 molecules, 21,852,845 ring systems, and 4,401,506
161 functional groups. The distribution of the occurrence frequency of these ring systems and
162 functional groups is shown in Figure 1. Figure 1 indicates that ~80% of ring systems and ~66%
163 functional groups in GDB-13 occur in compounds only 1-2 times, while only ~1% of ring systems
164 and functional groups are observed in GDB-13 molecules more than 200 times. In general, most
165 of the ring systems (~93%) and functional groups (~91%) appear in GDB-13 less than 20 times.



166
167 **Figure 1.** Distribution of ring systems (RS) and functional groups (FG) in GDB-13 according to
168 the frequency of occurrence. Y-axis is the percentage plotted on a logarithmic scale.

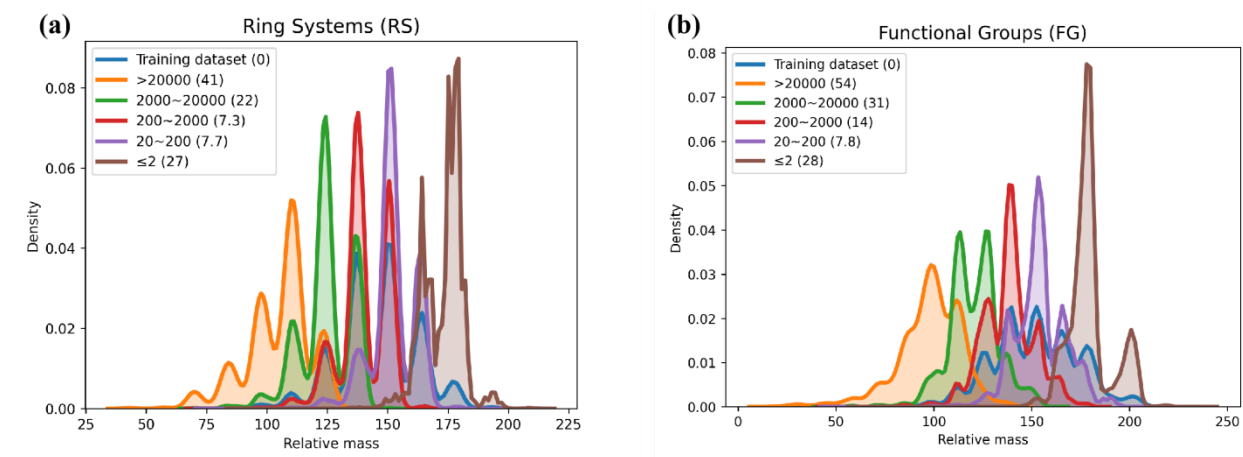
169 Analysis of the 1M training dataset

170 One million SMILES were randomly selected from the GDB-13 database for the training set,
171 which corresponds to roughly 0.1% of the total GDB-13 dataset. The training set contains around
172 0.9% of the ring systems and functional groups in the whole GDB-13 database (Table 1). The
173 coverage of the ring systems and functional groups is nine times as high as the coverage of
174 compounds, which is obviously due to the fact that some ring systems and functional groups occur
175 far more than once in GDB-13, as shown in Figure 1.

176 **Table 1.** Summary of GDB-13 coverage in the training set, consisting of 1M randomly selected
177 molecules.

Item	Counts in the training dataset (1M)	Coverage of GDB-13
Compounds	1,000,000	~0.1%
Ring systems	202,848	~0.9%
Functional groups	38,209	~0.9%

178



179

180 **Figure 2.** The fragment weight distributions for the different substructures in GDB-13. The different
181 colors indicate distributions involving substructures that occur in GDB-13 a similar number of
182 times (i.e. orange is substructures that occur >20,000 times in GDB-13, brown is substructures that

183 occur ≤ 2 times). In the key, the numbers in parentheses indicate the Wasserstein distance between
184 the training set distribution and the indicated distribution. (a) Ring systems (RS). (b) Functional
185 groups (FG).

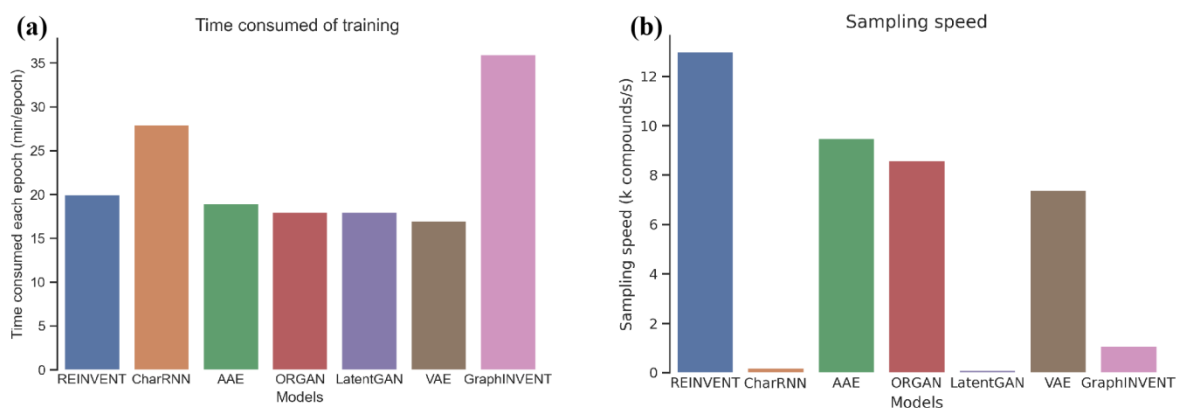
186 The fragment weights (FWs) of ring systems and functional groups in the training set, grouped by
187 frequency of occurrence, are shown in Figure 2. The FWs here were calculated from the
188 composition of specific ring systems and functional groups rather than the full compound. It is
189 observed that their probability of occurrence decreases with increasing FW. For example, the mean
190 FW of RS and FG which occur with a frequency $>20,000$ is around 100; however, for RS and FG
191 which occur ≤ 2 times in GDB-13, the mean FW is around 170. More basic RS and FG, such as
192 C1CC1 (cyclopropyl) and C=O (carbonyl), respectively, tend to have smaller FW compared to
193 complex RS and FG. Furthermore, many complex RS and FG can be built from the basic
194 components via enumeration and combination following the chemical rules extracted from the
195 training dataset.

196 **Training and sampling speed**

197 All deep molecular generative models were trained with the same training set of 1M compounds.
198 Each epoch of training took 17-20 min for most models (Figure 3), except CharRNN (28 min) and
199 GraphINVENT (36 min). In general, the training speed of all the models is acceptable. We
200 observed that training SMILES-based models is faster than the graph-based model; this is
201 understandable because the action space of the graph-based model is much larger than any of the
202 SMILES-based models.

203 Nonetheless, the sampling speed of the generative models was observed to vary significantly. The
204 sampling speed of REINVENT, AAE, ORGAN, and VAE were all above 7000 compounds per
205 second, while the sampling speed of CharRNN, LatentGAN, and GraphINVENT were only 200,

206 100, and 1100 compounds per second, respectively. Notably, CharRNN and REINVENT share
207 similar architecture of character-level recurrent neural networks. The difference of their
208 performance is mainly due to CharRNN implementation provided by MOSES adopts a larger size
209 of architecture. The detailed hyper parameters are given as Table S2 in the supporting materials.
210 It should also be noted that both training and sampling speeds are strongly related to the batch size
211 that is limited by the memory of the GPU. In current work, the default batch size as specified in
212 the code was used during the training, while for sampling, the largest batch size allowed by the
213 GPU memory was chosen.
214 Given the relatively small size of the training set (1M molecules), all the deep generative models
215 had a tractable training speed. In terms of sampling, the sampling speed was limited by each
216 model's architecture and size; using a larger sampling batch size allowed by a greater GPU
217 memory could boost the sampling speed.



218 **Figure 3.** Training and sampling speeds of the generative models benchmarked in this work. (a)
219 Time consumed per epoch during training. (b) Sampling speed, which is the number of
220 SMILES/graphs generated per second (including invalid ones).
221

222 **Validity and repetition rate of sampled molecules**

223 We first check the validity of the molecules generated by all the deep generative models, which is
224 defined as the percentage of chemically valid SMILES/graphs in the 1B generated set. Table 2
225 shows that the validity in general is satisfactory for all models, where most models achieve a
226 validity higher than 90 percent. RNN based models (REINVENT and CharRNN) have the highest
227 validity which is above 99.3% (Table 2). The validity of LatentGAN and GraphINVENT are 85.4%
228 and 95.3% respectively, which are lowest among all the models. In order to check how much
229 duplication is generated among the sample sets, the repetition rate (R_{rept}) was calculated via the
230 formula below:

$$231 \quad R_{rept} = \frac{N_{valid} - N_{unique}}{N_{unique}}, \quad (1)$$

232 where, N_{valid} is the number of total valid molecules in the 1B generated set and N_{unique} is the
233 number of unique valid molecules in the 1B generated set (i.e. duplicates removed). The compound
234 repetition rates of most deep generative models were around 1.0, that is to say, most compounds
235 were sampled twice on the average. ORGAN and CharRNN have the highest repetition rates,
236 which are 3.8 and 1.4 respectively, whereas GraphINVENT and LatentGAN have the lowest (0.7).
237 It seems that all the deep generative models had a satisfactory high percent validity that was above
238 85% in this study. The validity of CharRNN reached as high as 99.7%. ORGAN had a repetitive
239 rate as high as 3.8, which means that each generated compound was sampled 4.8 times on average.
240 The high repetition rate resulted in a low overall compound coverage for ORGAN, where the
241 coverage was as low as 16%.

242 **Table 2.** Percentage of the valid molecules and molecular repetition rate in the 1B generated set
243 for each model in this study. The uncertainty in the percent validity was less than a fraction of a
244 percentage point for each model.

Model	REINVENT	CharRNN	AAE	ORGAN	LatentGAN	VAE	GraphINVENT
Validity (%)	99.3	99.7	97.8	97.2	85.4	98.2	95.3
Repetition rate	0.9	1.4	0.9	3.8	0.7	1.0	0.7

245

246 Coverage of GDB-13 chemical space

247 The molecule and substructure coverage of GDB-13 space for all generative models studied herein
 248 is shown in Figure 4a. It can be seen that all the models possess good capabilities for generalization,
 249 surpassing the coverage of the 1M training set used, which has a ~0.1% coverage of GDB-13
 250 compounds, ~0.9% coverage of GDB-13 ring systems, and ~0.9% coverage of GDB-13 functional
 251 groups. REINVENT achieves the highest compound and FG coverage (39% and 26%,
 252 respectively), while AAE achieves best RS coverage (41%). The GAN models (ORGAN and
 253 LatentGAN) have lowest coverage at all three levels.

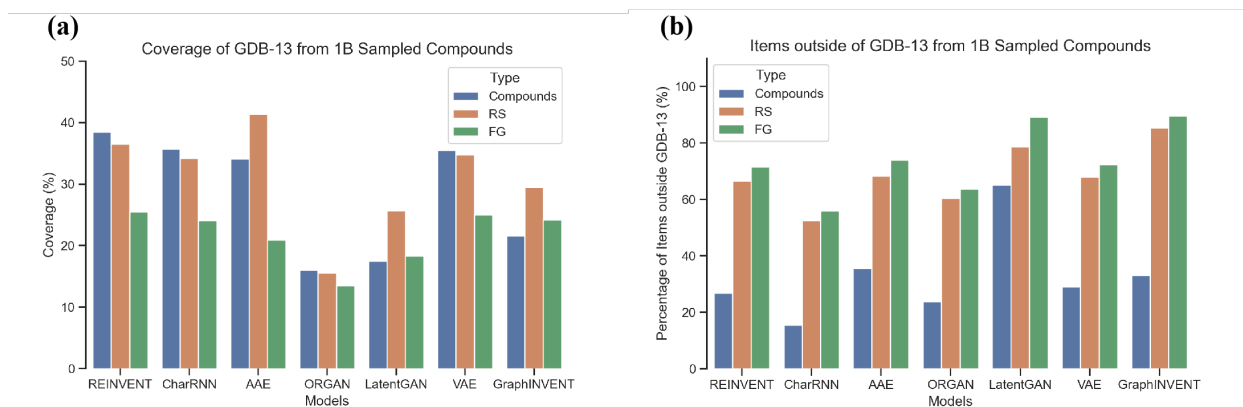
254 Using these new metrics, the difference in performance among these models is more pronounced;
 255 this is in contrast to a previous benchmarking study using the MOSES metrics,⁽¹⁰⁾ where the two
 256 GAN models appear to perform similarly with the CharRNN, AAE, and VAE models.

257 Overall, REINVENT, CharRNN, AAE, and VAE are the top-ranking models in this benchmarking
 258 study. They have a compound coverage, RS coverage, and FG coverage around 34%, 34%, and
 259 21%, respectively, in all cases. The performance of GraphINVENT is in the middle rank among
 260 the generative models in this study, and demonstrates coverage scores of 22%, 30%, and 24% for
 261 compound coverage, RS coverage, and FG coverage, respectively.

262

263

264



266

267 **Figure 4.** Coverage of GDB-13 chemical space using 1B sampled molecules. (a) Coverage of
 268 compounds, ring systems (RS), and functional groups (FG) in GDB-13 ($P_{covered}$). (b) Percentage
 269 of sampled molecules, RS, and FG that are outside the chemical space of GDB-13 (P_{out}).

270 Coverage of compounds, RS, and FG in GDB-13 was calculated via the formula below:

$$271 \quad P_{covered} = \frac{N_{unique_in}}{N_{GDB13}} * 100\%, \quad (2)$$

272 where N_{unique_in} is the number of unique valid sampled compounds, RS, or FG that are also found
 273 in GDB-13, and N_{GDB13} is the total number of compounds, RS, or FG present in GDB-13.

274 The percentage of sampled compounds, RS, or FG that are outside the chemical space of GDB-13
 275 was calculated via the formula below:

$$276 \quad P_{out} = \frac{N_{unique_out}}{N_{unique}} * 100\%, \quad (3)$$

277 where N_{unique_out} is the number of unique valid sampled compounds, RS, or FG that are *not* found
 278 in GDB-13, and N_{unique} is the total number of unique valid compounds, RS, or FG in the generated
 279 sets.

280 There are four major metrics mentioned above, namely validity, repetition rate, coverage of GDB-
281 13 chemical space, and percentage outside GDB-13. Validity represents how good a generative
282 model has learned the chemical rules for constructing compounds; repetition rate represents how
283 much structure duplication exists in the generated compound set; generalization capacities of
284 models can be measured with the coverage of GDB-13 after being trained on a smaller fraction of
285 chemical space. As a supplement to above metrics, percentage outside GDB-13 shows how many
286 sampled compounds fall outside the scope of GDB-13 (which are usually non drug-like
287 compounds). Also, these four metrics are not independent from each other. For example, if a model
288 has a high validity and a small percentage sampled outside GDB-13, given that exactly 1B
289 compounds are sampled, the only reasonable explanation for a low GDB-13 coverage is a high
290 repetition rate.

291 Figure 4b shows the generated structures outside GDB-13. As GDB-13 uses filters to remove
292 molecules that do not satisfy simple chemical stability and synthetic feasibility rules, such as ring-
293 strain criteria and valency rules, there are many structures that can be generated which violate the
294 filters used by GDB-13. For example, there are around 27% valid SMILES generated by
295 REINVENT which fall outside the scope of GDB-13 chemical space. However, for CharRNN,
296 only 15% of its respective generated sets fall outside GDB-13, which is lower than other models
297 in this study. As the percent validity of the structures generated by both models is above 97%, we
298 conclude that the lower fraction of compounds outside GDB-13 is due to the high repetition rate
299 of compounds for these models, as shown in Table 2. As for the percentage of RS and FG outside
300 of the scope of GDB-13, more than 50% of all FG and RS found in the generated sets for each
301 model are outside the GDB-13 chemical space.

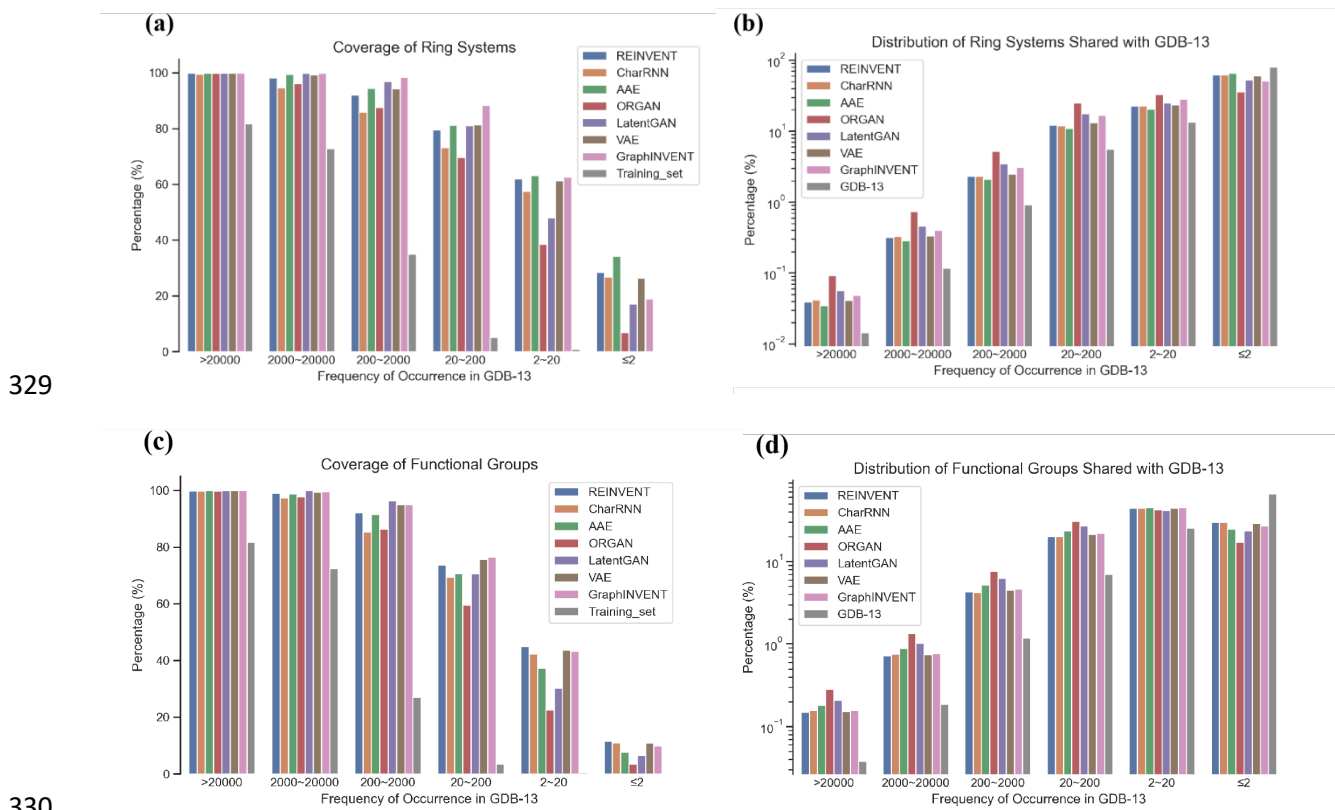
302 After training with a subset of the GDB-13 database (0.1%), all the generative models showed
303 promising performance in terms of compound coverage. Around 16% compounds of GDB-13 were
304 covered with 1B SMILES sampled by the LatentGAN, which is 160 times greater than the
305 coverage of the training dataset itself. The model with the best performance in this study is
306 REINVENT, which has an observed compound coverage as high as 39%. Thus, we conclude that
307 deep generative models in general have satisfactory learning and generalization capacities. In
308 terms of overall GDB-13 compound coverage, the rank of performance in descending order is
309 REINVENT > CharRNN > VAE > AAE > GraphINVENT > LatentGAN > ORGAN.

310 The GDB-13 coverage of RS and FG was generally less than the coverage of compounds, except
311 in the cases of AAE, LatentGAN, and GraphINVENT. However, in these cases, greater than 60%
312 RS and FG in the generated set were outside the scope GDB-13 chemical space, while less than
313 40% of generated molecules were outside GDB-13 (except LatentGAN). In terms of RS coverage
314 of GDB-13, the rank of performance in descending order is AAE > REINVENT > VAE >
315 CharRNN > GraphINVENT > LatentGAN > ORGAN. In terms of FG coverage of GDB-13, the
316 rank of performance in descending order is REINVENT > VAE > GraphINVENT > CharRNN >
317 AAE > LatentGAN > ORGAN. Examples of the most commonly observed groups in structures
318 generated by the two best models in terms of functional groups and ring systems recovery,
319 REINVENT and AAE, are shown in Figures 6 & 8. Examples of the most commonly observed
320 groups that are outside of GDB-13 in structures and generated by LatentGAN, are shown in Figures
321 7 & 9.

322 It is worthwhile to mention that the original LatentGAN adopts a heteroencoder and decoder model
323 (DDC) trained on ChEMBL dataset, the LatentGAN had a compounds coverage, RS coverage and
324 FG coverage of GDB-13 as 13%, 15% and 18%, respectively. When the DDC model were trained

325 on a 3M subset of GDB-13 instead, the compounds coverage, RS coverage and FG coverage of
326 GDB-13 increased to 18%, 26% and 18%, respectively. Thus, we adopted the heteroencoder and
327 decoder model trained on the 3M subset in this study.

328 Relationship between the coverage of GDB-13 and occurrence frequency



331 **Figure 5.** Coverage of GDB-13 chemical space from 1B sampled molecules, grouped by the
332 occurrence frequency of molecules in GDB-13. (a & c) Coverage of RS and FG. (b & d)
333 Distribution of generated RS and FG that are shared with the chemical space of GDB-13. The y-
334 axes for (b) and (d) are displayed in logarithmic scale.

335 The coverage of GDB-13 chemical space from 1B sampled molecules, grouped by the
336 occurrence frequency of molecules in GDB-13, was calculated via the formula below:

337
$$P_{covered} = \frac{N_{unique_in}(R_m, R_n)}{N_{GDB13}(R_m, R_n)} * 100\% , \quad (4)$$

338 where $N_{unique_in}(R_m, R_n)$ is the number of unique RS or FG in the sampled set that have an
339 occurrence frequency in the interval of $R_m - R_n$ (including R_n) in GDB-13, and $N_{GDB13}(R_m, R_n)$
340 is the total number of RS or FG in GDB-13 with an occurrence frequency in the interval of $R_m -$
341 R_n (including R_n). As such, $P_{covered}$ represents the coverage of specific set of substructures
342 $N_{GDB13}(R_m, R_n)$ of GDB-13 from the 1B generated set.

343 In Figures 5a and 5c, the RS and FG coverage of various models is broken down into different
344 frequency sections to examine the coverage performance for different types of substructures.
345 Figure 5 shows that for high frequency RS and FG, the coverage is high and quite similar among
346 all models, while for less frequent RS and FG, the coverage reveals differences between models.
347 On the other hand, comparing with the training set, all models demonstrate clear enrichment of RS
348 and FG coverage, and the enrichment gets bigger as the RS and FG frequency is lower. As for RS
349 and FG at the occurrence ranges of “>20000”, “2000-20000”, and “200-2000”, the coverage is
350 close to 100% for all models, while the coverage of the training dataset is around 82%, 73%, and
351 31% at these respective occurrence frequency ranges. As for RS at the occurrence range of “20-
352 200”, “2-20” and “≤2”, most generative models have an RS coverage of around 80%, 60%, and
353 30%, compared to only 5%, 1%, and 0% for the training dataset. The coverage of FG at the
354 different occurrence frequency ranges has a similar pattern to the RS coverage.

355 Similarly, distribution of generated RS and FG that are shared with the chemical space of GDB-
356 13 was calculated via the formula below:

357
$$P_{dist} = \frac{N_{unique_in}(R_m, R_n)}{N_{unique_in}} * 100\% , \quad (5)$$

358 where $N_{unique_in}(R_m, R_n)$ is the number of unique RS or FG in the sampled set that have an
359 occurrence frequency in the range of R_m to R_n in GDB-13, and N_{unique_in} is the total number of
360 unique RS or FG in the generated set, which are also included in GDB-13. Thus, P_{dist} is a metric
361 of the distribution of RS or FG that are shared with GDB-13 at different occurrence ranges.
362 The distributions of generated RS and FG corresponding to occurrence frequency in GDB-13 are
363 shown in Figures 5b & 5d. Given that most RS and FG have an occurrence frequency below 20 in
364 the GDB-13 database (as shown in Figure 1), the overall coverage of RS and FG is thus dominated
365 by ones with low occurrence frequency.
366 The most frequent and least frequent ring systems and functional groups sampled by the deep
367 generative models are listed in Figures 6-9. The most often sampled ring systems are simple carbon
368 cycles or aromatic heterocycles containing O and N atoms, such as C1CC1 (cyclopropane), which
369 was sampled up to 78M times in the 1B sample set, and C1COC1 (oxetane), which were sampled
370 up to 26M times in the 1B sample set. For comparison, the benzene ring ranked 85th among the
371 most common sampled ring systems. As for the least common sampled ring systems, they were
372 usually complex macrocycles that were only sampled once out of the 1B compounds generated.
373 The most commonly sampled functional groups are ordinary small ones, such as single oxygen
374 and nitrogen atoms, C-C double bonds, and C-C triple bonds. The least commonly sampled
375 functional groups are those with complex structures formed by a combination of simple ones. The
376 ring systems and functional groups that are not included in GDB-13 usually do not conform to
377 simple chemical stability and synthetic feasibility rules.
378 Most of the RS (~93%) and FG (~91%) found in the generated sets that are also found in GDB-13
379 are seen less than 20 times. As the results show in Figure 2, RS and FG that occur more frequently
380 in GDB-13 tend to have smaller fragment weights. The building blocks of RS and FG are basic

381 rings and functional groups with simple structures and small fragment weights. More complex RS
382 and FG can be built via the combination of these basic components.

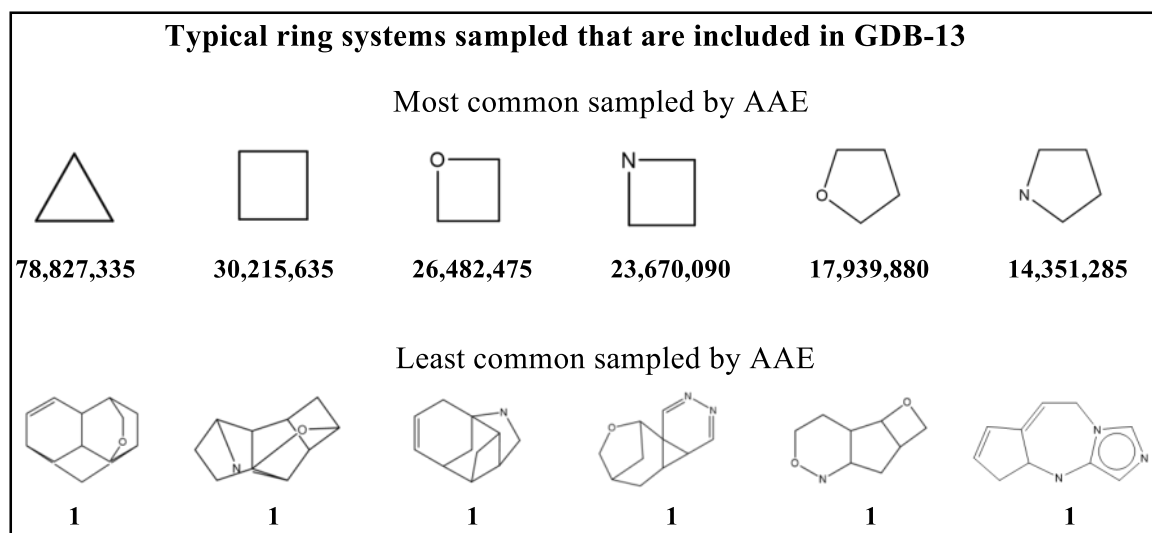
383 The coverage of RS and FG with an occurrence frequency in GDB-13 greater than 200 was nearly
384 100%. This is because these RS and FG can be easily obtained via combinations of smaller
385 fragments. However, given that as many as up to 13 heavy atoms were considered in constructing
386 the GDB-13 database, most RS and FG possess complex structures and were included in
387 compounds of GDB-13 less than 20 times. RS and FG that occur less than 20 times in the generated
388 sets dominate the coverage of the deep generative models.

389 Besides, as shown in Figures 10, most common ring systems and functional groups sampled by
390 generative models have close relative occurrence frequency compared to their distribution in
391 GDB-13.

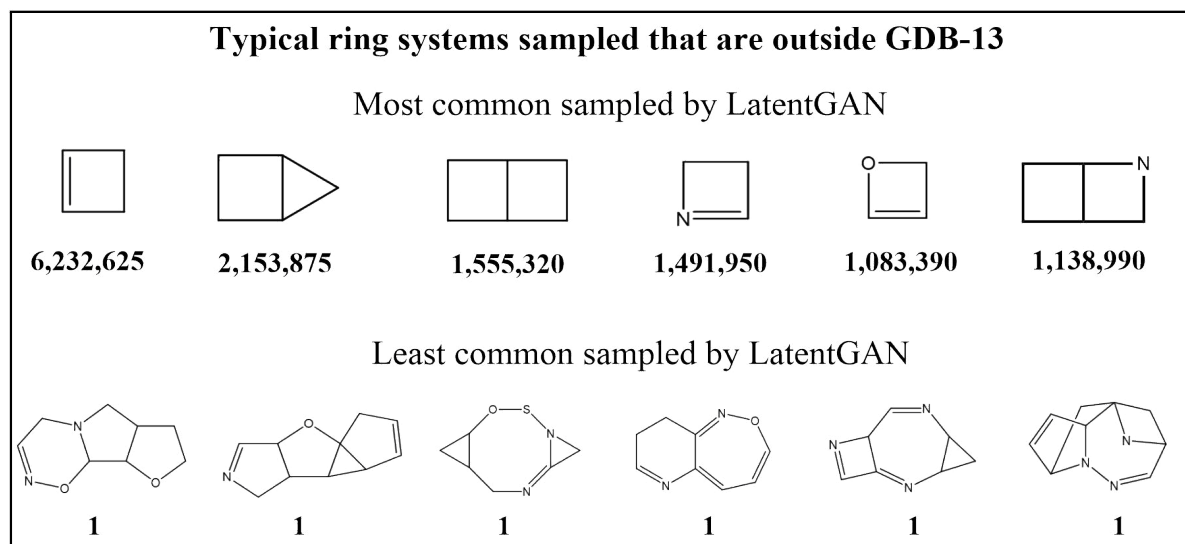
392 **Model comparison**

393 It is interesting to observe that these models describe the chemical space so differently, although
394 trained with the same training set. It seems that the RS and FG coverage of GraphINVENT is
395 higher than its overall molecular coverage, one reason could be due to its large action space; that
396 is, the number of possible “correct” sampled actions at any stage during graph generation is much
397 larger than it is for SMILES-based methods which must use only tokens sampled in the training
398 set. As such, given that GraphINVENT samples actions probabilistically, it is possible that
399 sequences of actions are sampled which have never been seen in the training set, thus leading to
400 new molecules. Another interesting observation is that GAN based models generally perform
401 worst in terms of GDB-13 coverage on all three metrics, one reason could be due to that, in the
402 adversarial training, the generator is supposed to mimic the true data as much as possible to fool
403 the discriminator, which deteriorates its generalization capability to a certain extent. We also

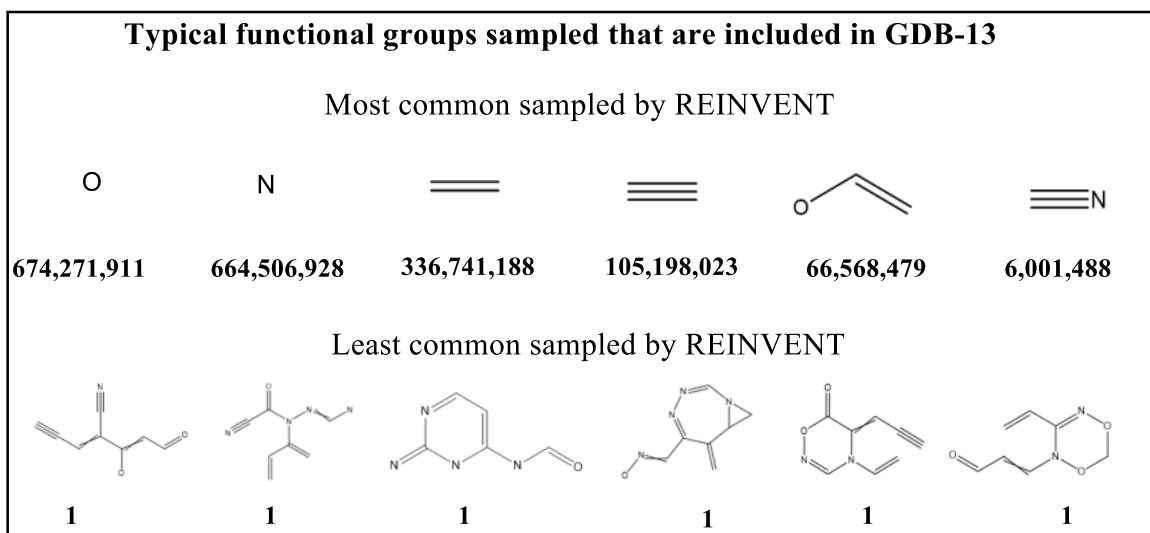
404 noticed that the performance of REINVENT and CharRNN is somehow similar, while their
 405 sampling speed has very large difference. Given that both models are based on the same RNN
 406 architecture, suggesting that the technical implementation of CharRNN is suboptimal.



407
 408 **Figure 6.** Typical ring systems that are sampled by AAE, which are included in GDB-13. The
 409 numbers below the structures in the figure are the occurrence frequency of ring systems in the 1B
 410 sampled compounds.



411
 412 **Figure 7.** Typical ring systems that are sampled by LatentGAN, which are outside GDB-13.

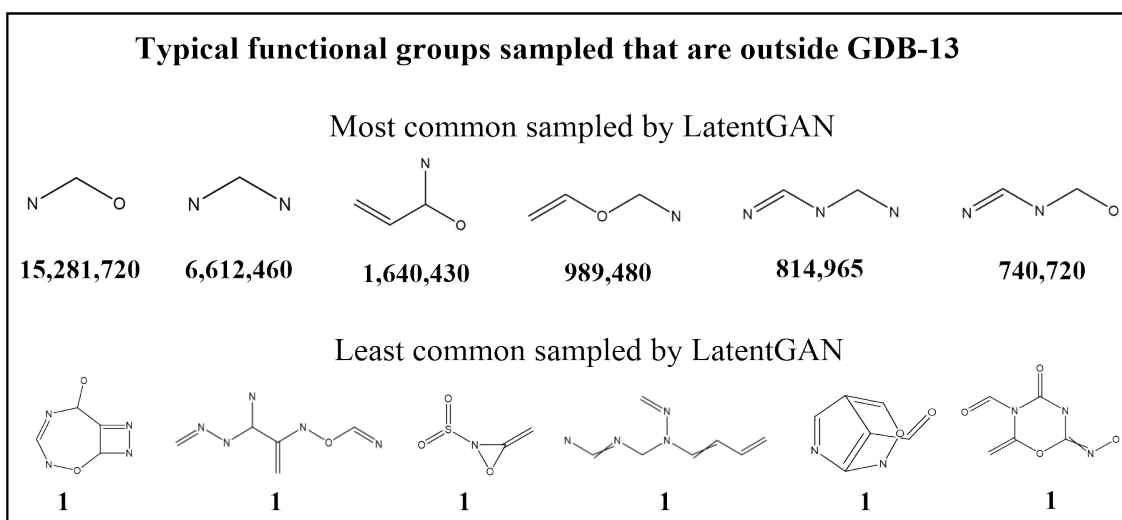


413

414 **Figure 8.** Typical functional groups that are sampled by REINVENT, which are included in GDB-

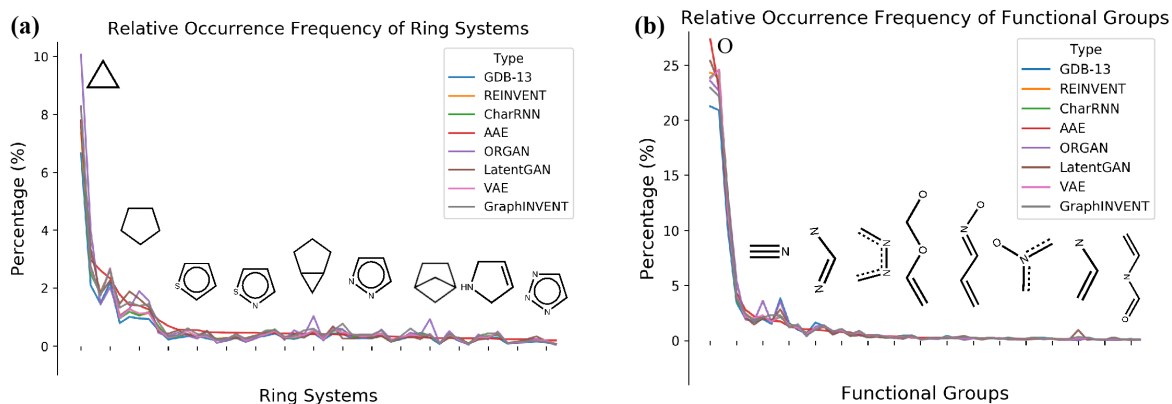
415 13.

416



417

418 **Figure 9.** Typical functional groups that are sampled by LatentGAN, which are outside GDB-13.



419

420 **Figure 10.** Relative occurrence frequency of most common functional groups and ring systems.

421 Conclusions

422 Molecules consist of a variety of ring systems and functional groups, which are connected in
 423 different ways to form molecules. The most basic ring systems and functional groups have simple
 424 structures and small fragment weights; these can be found in GDB-13 molecules over dozens of
 425 times. More complex ring systems and functional groups have complicated structures and large
 426 fragment weights, and might only occur in GDB-13 a handful of times. However, due to their
 427 structural variety and enormous quantity (>90%), complex ring systems and functional groups are
 428 strong components affecting the coverage of GDB-13.

429 All the deep generative models studied in this work have over 100 times greater chemical space
 430 coverage for GDB-13 using 1B samples than the training set (1M) used to train the models. In
 431 terms of compound coverage of GDB-13, the best model (REINVENT) reached ~39% coverage,
 432 far beyond the coverage of ORGAN (~16%), which ranked lowest amongst the models in this
 433 study. Depending on the generative task, the deep generative model used should thus be chosen

434 carefully, as there are differences in how all these seemingly similar models sample the chemical
435 space.

436 **Associated Content**

437 **Author Information**

438 **Corresponding Author**

439 Hongming Chen, E-mail: chen_hongming@grmh-gdl.cn

440 **Author Contributions**

441 J. Z. ran training and generation jobs using REINVENT, CharRNN, VAE; LatentGAN, and
442 ORGAN. R. M. ran training and generation jobs using GraphINVENT. R. M. and J. Z. ran
443 benchmarking calculations for this work, and J. Z. made all figures. The manuscript was written
444 through the contributions of all authors. All authors have given approval to the final version of the
445 manuscript.

446 **Acknowledgements**

447 J. Z. would like to acknowledge funding provided by XtalPi Inc, and R. M. thanks the Postdoc
448 Program at AstraZeneca.

449 **Supplementary Materials**

450 The detailed hyperparameters and training loss curves of all models can be found in supplementary
451 materials. The training, sampling, and analysis script could found in the GitHub repository,
452 https://github.com/jeah-z/Generative_Models_benchmark_gdb13.

453 **Abbreviations**

454 RS, Ring system(s); FG, Functional group(s); GAN, Generative adversarial network; GNN,
455 graph neural network; RNN, recurrent neural network.

456 **References**

- 457 (1) Ciregan, D.; Meier, U.; Schmidhuber, J. Multi-Column Deep Neural Networks for Image Classification.
458 In 2012 IEEE conference on computer vision and pattern recognition, 2012; IEEE: 2012; pp 3642-3649.
- 459 (2) Krizhevsky, A.; Sutskever, I.; Hinton, G. E. Imagenet Classification with Deep Convolutional Neural
460 Networks. In Advances in neural information processing systems, 2012; 2012; pp 1097-1105.
- 461 (3) Taigman, Y.; Yang, M.; Ranzato, M. A.; Wolf, L. Deepface: Closing the Gap to Human-Level Performance
462 in Face Verification. In Proceedings of the IEEE conference on computer vision and pattern recognition,
463 2014; 2014; pp 1701-1708.
- 464 (4) Silver, D.; Huang, A.; Maddison, C. J.; Guez, A.; Sifre, L.; Van Den Driessche, G.; Schrittwieser, J.;
465 Antonoglou, I.; Panneershelvam, V.; Lanctot, M., Mastering the Game of Go with Deep Neural Networks
466 and Tree Search. *nature* **2016**, *529*, 484-489.
- 467 (5) Hadjeres, G.; Pachet, F.; Nielsen, F. Deepbach: A Steerable Model for Bach Chorales Generation. In
468 International Conference on Machine Learning, 2017; PMLR: 2017; pp 1362-1371.
- 469 (6) Garg, S.; Rish, I.; Cecchi, G.; Lozano, A., Neurogenesis-Inspired Dictionary Learning: Online Model
470 Adaption in a Changing World. *arXiv preprint arXiv:1701.06106* **2017**.
- 471 (7) Johnson, M.; Schuster, M.; Le, Q. V.; Krikun, M.; Wu, Y.; Chen, Z.; Thorat, N.; Viégas, F.; Wattenberg,
472 M.; Corrado, G., Google's Multilingual Neural Machine Translation System: Enabling Zero-Shot Translation.
473 *Transactions of the Association for Computational Linguistics* **2017**, *5*, 339-351.
- 474 (8) Bjerrum, E. J.; Threlfall, R., Molecular Generation with Recurrent Neural Networks (Rnns). *arXiv*
475 *preprint arXiv:1705.04612* **2017**.
- 476 (9) Kotsias, P.-C.; Arús-Pous, J.; Chen, H.; Engkvist, O.; Tyrchan, C.; Bjerrum, E. J., Direct Steering of De
477 Novo Molecular Generation with Descriptor Conditional Recurrent Neural Networks. *Nature Machine*
478 *Intelligence* **2020**, *2*, 254-265.
- 479 (10) Polykovskiy, D.; Zhebrak, A.; Sanchez-Lengeling, B.; Golovanov, S.; Tatanov, O.; Belyaev, S.; Kurbanov,
480 R.; Artamonov, A.; Aladinskiy, V.; Veselov, M.; Kadurin, A.; Johansson, S.; Chen, H.; Nikolenko, S.; Aspuru-
481 Guzik, A.; Zhavoronkov, A., Molecular Sets (Moses): A Benchmarking Platform for Molecular Generation
482 Models. *Front Pharmacol* **2020**, *11*, 565644.
- 483 (11) Prykhodko, O.; Johansson, S. V.; Kotsias, P.-C.; Arús-Pous, J.; Bjerrum, E. J.; Engkvist, O.; Chen, H., A
484 De Novo Molecular Generation Method Using Latent Vector Based Generative Adversarial Network.
485 *Journal of Cheminformatics* **2019**, *11*, 74.
- 486 (12) Schneider, G.; Fechner, U., Computer-Based De Novo Design of Drug-Like Molecules. *Nat Rev Drug*
487 *Discov* **2005**, *4*, 649-63.
- 488 (13) DiMasi, J. A.; Grabowski, H. G.; Hansen, R. W., Innovation in the Pharmaceutical Industry: New
489 Estimates of R&D Costs. *Journal of health economics* **2016**, *47*, 20-33.
- 490 (14) Patel, H.; Bodkin, M. J.; Chen, B.; Gillet, V. J., Knowledge-Based Approach to De Novo Design Using
491 Reaction Vectors. *Journal of chemical information and modeling* **2009**, *49*, 1163-1184.
- 492 (15) Schneider, G.; Lee, M.-L.; Stahl, M.; Schneider, P., De Novo Design of Molecular Architectures by
493 Evolutionary Assembly of Drug-Derived Building Blocks. *Journal of computer-aided molecular design* **2000**,
494 *14*, 487-494.
- 495 (16) Spiegel, J. O.; Durrant, J. D., Autogrow4: An Open-Source Genetic Algorithm for De Novo Drug Design
496 and Lead Optimization. *Journal of Cheminformatics* **2020**, *12*, 1-16.

497 (17) Chen, H.; Engkvist, O.; Wang, Y.; Olivecrona, M.; Blaschke, T., The Rise of Deep Learning in Drug
498 Discovery. *Drug discovery today* **2018**, *23*, 1241-1250.

499 (18) Blaschke, T.; Arus-Pous, J.; Chen, H.; Margreitter, C.; Tyrchan, C.; Engkvist, O.; Papadopoulos, K.;
500 Patronov, A., Reinvent 2.0: An Ai Tool for De Novo Drug Design. *J Chem Inf Model* **2020**, *60*, 5918-5922.

501 (19) Blaschke, T.; Olivecrona, M.; Engkvist, O.; Bajorath, J.; Chen, H., Application of Generative
502 Autoencoder in De Novo Molecular Design. *Molecular informatics* **2018**, *37*, 1700123.

503 (20) Guimaraes, G. L.; Sanchez-Lengeling, B.; Outeiral, C.; Farias, P. L. C.; Aspuru-Guzik, A., Objective-
504 Reinforced Generative Adversarial Networks (Organ) for Sequence Generation Models. *arXiv preprint*
505 *arXiv:1705.10843* **2017**.

506 (21) Kadurin, A.; Aliper, A.; Kazennov, A.; Mamoshina, P.; Vanhaelen, Q.; Khrabrov, K.; Zhavoronkov, A.,
507 The Cornucopia of Meaningful Leads: Applying Deep Adversarial Autoencoders for New Molecule
508 Development in Oncology. *Oncotarget* **2017**, *8*, 10883.

509 (22) Grisoni, F.; Moret, M.; Lingwood, R.; Schneider, G., Bidirectional Molecule Generation with Recurrent
510 Neural Networks. *Journal of chemical information and modeling* **2020**, *60*, 1175-1183.

511 (23) Gupta, A.; Müller, A. T.; Huisman, B. J.; Fuchs, J. A.; Schneider, P.; Schneider, G., Generative Recurrent
512 Networks for De Novo Drug Design. *Molecular informatics* **2018**, *37*, 1700111.

513 (24) Olivecrona, M.; Blaschke, T.; Engkvist, O.; Chen, H., Molecular De-Novo Design through Deep
514 Reinforcement Learning. *J Cheminform* **2017**, *9*, 48.

515 (25) Segler, M. H.; Kogej, T.; Tyrchan, C.; Waller, M. P., Generating Focused Molecule Libraries for Drug
516 Discovery with Recurrent Neural Networks. *ACS central science* **2018**, *4*, 120-131.

517 (26) Yuan, Q.; Santana-Bonilla, A.; Zwijnenburg, M. A.; Jelfs, K. E., Molecular Generation Targeting Desired
518 Electronic Properties Via Deep Generative Models. *Nanoscale* **2020**, *12*, 6744-6758.

519 (27) Kalchbrenner, N.; Grefenstette, E.; Blunsom, P., A Convolutional Neural Network for Modelling
520 Sentences. *arXiv preprint arXiv:1404.2188* **2014**.

521 (28) Kingma, D. P.; Welling, M., Auto-Encoding Variational Bayes. *arXiv preprint arXiv:1312.6114* **2013**.

522 (29) Kusner, M. J.; Paige, B.; Hernández-Lobato, J. M., Grammar Variational Autoencoder. *arXiv preprint*
523 *arXiv:1703.01925* **2017**.

524 (30) Brown, N.; Fiscato, M.; Segler, M. H.; Vaucher, A. C., Guacamol: Benchmarking Models for De Novo
525 Molecular Design. *Journal of chemical information and modeling* **2019**, *59*, 1096-1108.

526 (31) Blum, L. C.; Reymond, J.-L., 970 Million Druglike Small Molecules for Virtual Screening in the Chemical
527 Universe Database Gdb-13. *Journal of the American Chemical Society* **2009**, *131*, 8732-8733.

528 (32) Arus-Pous, J.; Blaschke, T.; Ulander, S.; Reymond, J. L.; Chen, H.; Engkvist, O., Exploring the Gdb-13
529 Chemical Space Using Deep Generative Models. *J Cheminform* **2019**, *11*, 20.

530 (33) Ertl, P.; Altmann, E.; McKenna, J. M., The Most Common Functional Groups in Bioactive Molecules
531 and How Their Popularity Has Evolved over Time. *Journal of Medicinal Chemistry* **2020**, *63*, 8408-8418.

532 (34) Taylor, R. D.; MacCoss, M.; Lawson, A. D., Rings in Drugs. *J Med Chem* **2014**, *57*, 5845-59.

533 (35) Arús-Pous, J.; Johansson, S. V.; Prykhodko, O.; Bjerrum, E. J.; Tyrchan, C.; Reymond, J.-L.; Chen, H.;
534 Engkvist, O., Randomized Smiles Strings Improve the Quality of Molecular Generative Models. *Journal of*
535 *Cheminformatics* **2019**, *11*.

536 (36) Gómez-Bombarelli, R.; Wei, J. N.; Duvenaud, D.; Hernández-Lobato, J. M.; Sánchez-Lengeling, B.;
537 Sheberla, D.; Aguilera-Iparraguirre, J.; Hirzel, T. D.; Adams, R. P.; Aspuru-Guzik, A., Automatic Chemical
538 Design Using a Data-Driven Continuous Representation of Molecules. *ACS central science* **2018**, *4*, 268-
539 276.

540 (37) Makhzani, A.; Shlens, J.; Jaitly, N.; Goodfellow, I.; Frey, B., Adversarial Autoencoders. *arXiv preprint*
541 *arXiv:1511.05644* **2015**.

542 (38) Mercado, R.; Rastemo, T.; Lindelöf, E.; Klambauer, G.; Engkvist, O.; Chen, H.; Bjerrum, E. J., Practical
543 Notes on Building Molecular Graph Generative Models. *ChemRxiv* **2020**, *Preprint*.

544 (39) Landrum, G., Rdkit: Open-Source Cheminformatics. **2006**.

- 545 (40) Ertl, P., An Algorithm to Identify Functional Groups in Organic Molecules. *Journal of cheminformatics*
546 **2017**, *9*, 1-7.
- 547 (41) Arús-Pous, J. Reinvent-Randomized. <https://github.com/undeadpixel/reinvent-randomized>
548 (accessed Sep 1, 2020).
- 549 (42) Polykovskiy, D.; Zhebrak, A.; Sanchez-Lengeling, B.; Golovanov, S.; Tatanov, O.; Belyaev, S.; Kurbanov,
550 R.; Artamonov, A.; Aladinskiy, V.; Veselov, M. Moses. <https://github.com/molecularsets/moses> (accessed
551 May 20, 2020).
- 552 (43) Johansson, S.; Prykhodko, O. Latent-Gan. <https://github.com/Dierme/latent-gan> (accessed Jan 5,
553 2021).
- 554 (44) Kotsias, P.; Bjerrum, E. J. Deepdrugcoder. <https://github.com/pcko1/Deep-Drug-Coder> (accessed Jan
555 5, 2021).
- 556 (45) Mercado, R.; Rastemo, T.; Lindelöf, E. Graphinvent. <https://github.com/MolecularAI/GraphINVENT/>
557 (accessed Oct 20, 2020).
- 558 (46) Rocío, M.; Tobias, R.; Edvard, L.; Günter, K.; Ola, E.; Hongming, C.; Esben Jannik, B., Graph Networks
559 for Molecular Design. *ChemRxiv* **2020**, *Preprint*.
- 560 (47) Oliphant, T. E., Python for Scientific Computing. *Computing in Science & Engineering* **2007**, *9*, 10-20.
- 561 (48) Paszke, A.; Gross, S.; Massa, F.; Lerer, A.; Bradbury, J.; Chanan, G.; Killeen, T.; Lin, Z.; Gimelshein, N.;
562 Antiga, L. Pytorch: An Imperative Style, High-Performance Deep Learning Library. In Advances in neural
563 information processing systems, 2019; 2019; pp 8026-8037.
- 564 (49) Panaretos, V. M.; Zemel, Y., Statistical Aspects of Wasserstein Distances. *Annual review of statistics*
565 *and its application* **2019**, *6*, 405-431.
- 566 (50) Virtanen, P.; Gommers, R.; Oliphant, T. E.; Haberland, M.; Reddy, T.; Cournapeau, D.; Burovski, E.;
567 Peterson, P.; Weckesser, W.; Bright, J., Scipy 1.0: Fundamental Algorithms for Scientific Computing in
568 Python. *Nature methods* **2020**, *17*, 261-272.

569

570

